




ORIGINAL RESEARCH

Kv1.3 Channel Inhibition Limits Uremia-Induced Calcification in Mouse and Human Vascular Smooth Muscle

Violeta Cazaña-Pérez^{1,2}, Pilar Ciudad³, Juan F. Navarro-González ², Jorge Rojo-Mencía³, Frederic Jaisser⁴, José R. López-López³, Diego Alvarez de la Rosa ¹, Teresa Giraldez ^{1,*}, Maria Teresa Pérez-García^{3,*}

¹Departamento de Ciencias Médicas Básicas (Fisiología), Instituto de Tecnologías Biomédicas, Universidad de La Laguna, Spain, ²Unidad de Investigación y Servicio de Nefrología, Hospital Universitario Nuestra Señora de Candelaria, Tenerife, Spain, ³Departamento de Bioquímica y Biología Molecular y Fisiología e Instituto de Biología y Genética Molecular (IBGM), Universidad de Valladolid y Consejo Superior de Investigaciones Científicas (CSIC), Valladolid, Spain and ⁴Unité Mixte de Recherche Scientifique 1138, Team 1, Institut National de la Santé et de la Recherche Médicale, Centre de Recherche des Cordeliers, La Laguna, Paris, France

*Address correspondence to M.T.P.-G. (e-mail: tperez@ibgm.uva.es), T.G. (e-mail: giraldez@ull.edu.es)

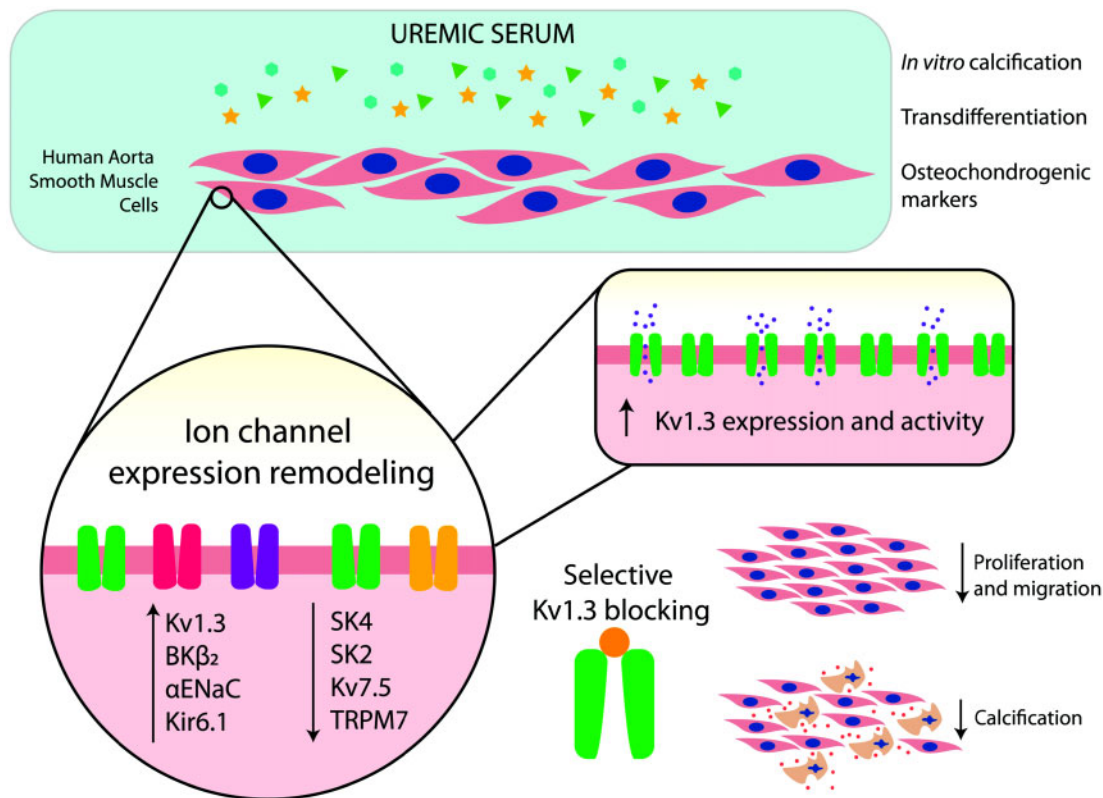
Abstract

Chronic kidney disease (CKD) significantly increases cardiovascular risk. In advanced CKD stages, accumulation of toxic circulating metabolites and mineral metabolism alterations triggers vascular calcification, characterized by vascular smooth muscle cell (VSMC) transdifferentiation and loss of the contractile phenotype. Phenotypic modulation of VSMC occurs with significant changes in gene expression. Even though ion channels are an integral component of VSMC function, the effects of uremia on ion channel remodeling has not been explored. We used an in vitro model of uremia-induced calcification of human aorta smooth muscle cells (HASMCs) to study the expression of 92 ion channel subunit genes. Uremic serum-induced extensive remodeling of ion channel expression consistent with loss of excitability but different from the one previously associated with transition from contractile to proliferative phenotypes. Among the ion channels tested, we found increased abundance and activity of voltage-dependent K⁺ channel Kv1.3. Enhanced Kv1.3 expression was also detected in aorta from a mouse model of CKD. Pharmacological inhibition or genetic ablation of Kv1.3 decreased the amount of calcium phosphate deposition induced by uremia, supporting an important role for this channel on uremia-induced VSMC calcification.

Submitted: 23 September 2020; **Revised:** 30 November 2020; **Accepted:** 3 December 2020

© The Author(s) 2020. Published by Oxford University Press on behalf of American Physiological Society.

This is an Open Access article distributed under the terms of the Creative Commons Attribution Non-Commercial License (<http://creativecommons.org/licenses/by-nc/4.0/>), which permits non-commercial re-use, distribution, and reproduction in any medium, provided the original work is properly cited. For commercial re-use, please contact journals.permissions@oup.com



Key words: chronic kidney disease; phenotypic switch; ion channel remodeling; BK channels; voltage-dependent potassium channels

Introduction

Chronic kidney disease (CKD) strongly associates with increased cardiovascular risk.^{1,2} Vascular medial calcification is an early event during CKD^{3,4} directly triggered by the uremic milieu and alterations in mineral metabolism.^{5,6} Medial calcification results from a complex set of active and highly regulated mechanisms that include apoptosis/necrosis of vascular smooth muscle cells (VSMCs)^{7–9} and their transdifferentiation to an osteochondrogenic phenotype.^{4,10–12} In addition, VSMC migration and differentiation also contribute to intima layer calcification associated with intima hyperplasia and atherosclerotic plaque formation.^{13–16}

CKD induces phenotypic modulation of VSMC, which loses contractility and adopts a highly proliferative state.¹⁷ Other pathways of transdifferentiation have been proposed, including senescent, osteochondrogenic, and adipogenic phenotypes.¹⁸ The change from contractile to synthetic phenotype implies extensive modification in gene expression.¹⁹ Coordinated changes in ion channel expression constitute an integral component of VSMC plasticity.^{20,21} However, little is known regarding ion channel expression changes during uremia-induced VSMC transdifferentiation and their possible role on vascular calcification. We recently characterized an *in vitro* calcification and osteochondrogenic transdifferentiation model using human

aortic smooth muscle cells (HASMCs) exposed to serum from uremic patients.¹⁰ This model displays rapid calcification, upregulation of osteochondrogenic markers and phenotypic remodeling, while preserving cell viability and proliferation.¹⁰ Here we took advantage of this model to study the effect of uremia on the expression of relevant ion channel subunits. Our results uncovered extensive ion channel remodeling that led us to study in detail the implication of voltage-dependent K⁺ channel Kv1.3 in the effects of uremia on HASMC. We present data supporting a role for Kv1.3 on uremia-induced changes in cell proliferation, but not in cell migration. Most importantly, we show that pharmacological or genetic blockade of Kv1.3 partially reverts uremia-induced calcification in HASMC and also in human or mouse vessels in organ culture.

Material and Methods

Human Uremic Serum

Patient and healthy donor sera were obtained at the Nephrology Service, Hospital Universitario Nuestra Señora de Candelaria (Tenerife, Spain). The studies were approved by the Hospital Ethics Committee and conformed to the latest revision of the Declaration of Helsinki. All subjects gave informed consent to participate. Collection criteria of serum samples have been

reported elsewhere.¹⁰ We used serum pools from 16 healthy donors or from 16 Stage 5D CKD patients. Biochemical study of individual serum samples confirmed the expected characteristics for healthy and uremic serum.¹⁰ After individual serum analysis, samples were then pooled, aliquoted, and stored at -80°C until use.

Primary Human VSMC Culture

Primary HASMC were obtained from Innoprot (Derio, Spain) and cultured as described.¹⁰ Confluent cells were treated with medium supplemented with 20% of control or uremic human serum for the indicated period of time. When applicable, the Kv1.3-specific inhibitors 5-(4-phenoxybutoxy) psoralen (PAP-1, Sigma-Aldrich) and margatoxin (MgTx) were used at 100 nM^{22,23} and 10 nM,²⁴ respectively. All experiments were performed using cells between Passages 3 and 5.

Organ Culture of Human and Mouse Arteries

Human mammary arteries (hMAs) belonging to the COLMAH collection (COlección de Muestras Arteriales Humanas, https://www.redheracles.net/plataformas/en_coleccion-muestras-arteriales-humanas.html) were obtained from donors undergoing heart bypass surgery at the Clinic Hospital of Valladolid after written informed consent. The procedures were approved by the Hospital Ethics Committee according to the Helsinki Declaration. Mouse aortas (mAs) were obtained from Kv1.3+/+ (WT) and Kv1.3-/- mice (Kv1.3-/-) from Jackson Laboratory. Mice were maintained by inbreeding crossing and housed under controlled conditions and free access to water and food in the animal facility of the School of Medicine of Valladolid. Procedures were approved by the Institutional Care and Use Committee of the University of Valladolid, in accordance with the European Community guiding principles regarding care and use of animals (Directive 2010/63/UE).

Human and mouse arterial rings were incubated in MEM culture medium (Gibco) with penicillin-streptomycin (100 U/mL each), 5 $\mu\text{g}/\text{mL}$ Fungizone, and 2 mmol/L-glutamine at 37°C in 5% CO_2 humidified atmosphere as previously described.²⁵ To induce calcification (positive control), rings were placed in 20% FBS with 2.5 mM phosphate ($\text{Na}_2\text{H}_2\text{PO}_4/\text{NaH}_2\text{PO}_4$, 2:1, pH 7.4). The experimental conditions used were 20% of control or uremic human serum in the absence or presence of 100 nM PAP-1 as indicated in each experiment. Sequential sections of the same artery were used for the different experimental conditions. Media was refreshed every 2 days, and after 10 days in culture, rings were fixed with 4% formaldehyde.

Mouse Model of CKD

C57BL/6 mice were kept in a room at 22°C with a 12:12 h light:dark cycle and had free access to water and standard rodent chow. Mice with subtotal nephrectomy (5/6 model of CKD) were generated as previously described.²⁶ Total RNA was extracted from aorta using TRIZOL reagent (Life Technologies). The use of live animals was approved by Comité d'éthique en Expérimentation Animale Charles Darwin—CEEACD, Paris, France, and conducted in accordance with European Union guidelines (European Directive, 2010/63/UE).

Quantification of Gene Expression

Total RNA was purified from cultured HASMC using a commercial kit (Total RNA Spin Plus, REAL). Ion channel subunit transcription

profiling was performed using a TaqMan[®] low-density array (Applied Biosystems) containing a user-defined collection of 92 test and three housekeeper genes (Table S1) as described previously.^{27,28} Each gene was included in duplicate. Expression of KCNA3 (encoding Kv1.3) was further confirmed by conventional qPCR using a specific Taqman probe.¹⁰ Relative quantification was performed using the $\Delta\Delta\text{Ct}$ method.²⁹ Two-way hierarchical agglomerative clustering was performed as described.²⁷

Patch-Clamp Recordings

HASMC ionic currents were recorded at room temperature using whole-cell patch-clamp as described.²⁷ Borosilicate glass patch pipettes were pulled to a resistance of 2–5 M Ω when filled with the internal solution (in mM: 10 HEPES, 125 KCl, 4 MgCl₂, 10 EGTA, 5 MgATP, pH 7.2). The bath solution contained (in mM): 10 HEPES, 141 NaCl, 4.7 KCl, 1.2 MgCl₂, 1.8 CaCl₂, 10 glucose, pH 7.4. Whole-cell currents were recorded using an Axopatch 200 patch-clamp amplifier, filtered at 2 kHz (-3 dB, four-pole Bessel filter), and sampled at 10 kHz. Recordings were digitized with a Digidata 1322A interface, driven by CLAMPEX 10 software (Molecular Devices). Current-voltage relationships were obtained from a holding potential of -80 mV by applying 2 s ramp depolarisations from -60 to $+120$ mV, every 10 s. Cell capacitance was calculated by integrating capacitive currents elicited by 10 mV hyperpolarizing pulses. Results are expressed as current density (pA/pF).

Cell Proliferation

HASMC proliferation was assessed by 5-ethynyl-2'-deoxyuridine (EdU) incorporation using a commercial kit (Click-iT[®] EdU, ThermoFisher Scientific) as described.^{10,30} Cells were incubated with 10 μM EdU and treated with control or uremic serum for 1, 6, 12, or 24 h and then fixed with 4% formaldehyde. Cell nuclei were counterstained using Hoechst 33342 (ThermoFisher Scientific). Quantification of EdU-positive nuclei was performed in 15 random fields.

Cell Migration

HASMC migration was examined as described.¹⁰ Briefly, cells were grown to confluence in 35 mm dishes with a silicon insert that separates two chambers (Ibidi GmbH) and treated with control or uremic serum for 48 h. The insert was then removed and culture medium changed to serum-free DMEM to prevent cell proliferation. Images were collected at 24, 48, 72, and 120 h after removal of the insert and analyzed using ImageJ (National Institutes of Health).³¹

Calcification

Cells were treated with control or uremic serum for 1 or 5 days, fixed in 10% formalin, washed, and stained with 1% alizarin red (Sigma-Aldrich) to detect deposition of calcium phosphate crystals.¹⁰ Cells were then dissolved in 10% acetic acid and dye concentration was quantified by absorption at 450 nm and normalized to protein content measured using the bicinchoninic acid method (BCA assay kit, Sigma-Aldrich).

Rings in organ culture (hMA and mA) were fixed and paraffin-embedded to obtain 7 μm sections, which were stained using Alizarin red (2%) for 4–5 min. To measure calcification 3–4 microphotographs from each ring were acquired from a Nikon Eclipse 90i microscope using a Nikon CCD camera. The percentage of alizarin red-stained area was analyzed using the ImageJ

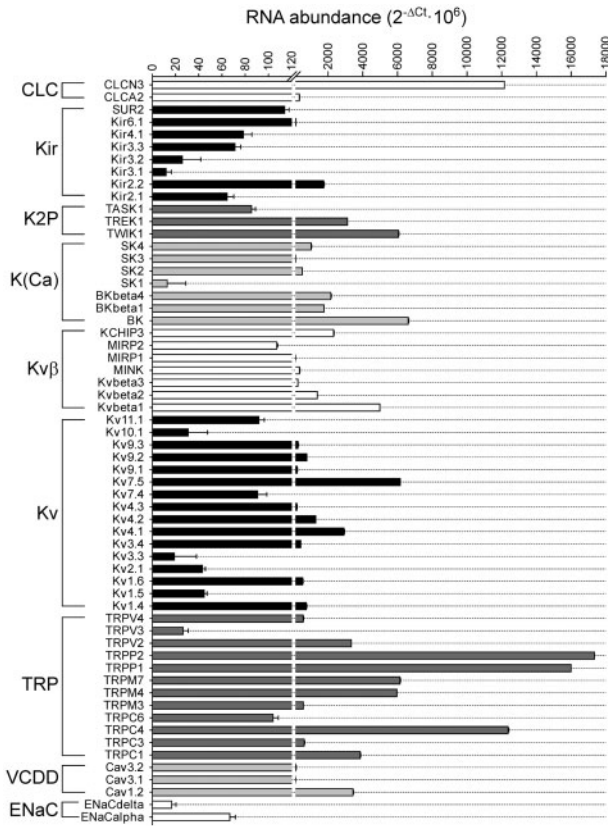


Figure 1. Relative mRNA Abundance of Ion Channels Genes in VSMCs (HASMC). HASMC were cultured in 20% control serum for 5 days. Expression levels were normalized to GAPDH and expressed as $2^{-\Delta Ct} \times 10^6$, where $\Delta Ct = Ct_{(gene)} - Ct_{(GAPDH)}$. Each bar is the mean of three independent samples analyzed in duplicate.

(Fiji) software. Both image selection and analysis were performed in a blind manner.

Statistical Analysis

Data were plotted and analyzed using Origin (OriginLab Corp., Northampton, MA, USA), Prims5 (GraphPad) and R software. Pooled data are expressed as mean \pm SEM, and P -values < 0.05 were considered as significantly different.

For comparisons between two groups with normal distribution, Student's t -test, for paired or unpaired data as required, was used to determined P -values, otherwise, Wilcoxon-Mann-Whitney (MMW) test (for paired or unpaired data) was applied. For comparisons among several groups, one-way ANOVA (ANalysis Of VAriance) followed by Tukey's test was employed in the case of normal distributions and equal variances; alternatively, Kruskal-Wallis analysis followed by Dunn's test was used. Shapiro-Wilk test and Bartlett's test were used to test normality and homogeneity of variances, respectively.

Results

Uremic Serum Induces Remodeling of Ion Channel Subunit Expression in HASMC

In order to obtain a global picture of ion channel subunit expression remodeling during uremia-induced HASMC phenotypic change, we used low-density TaqMan array analysis to study

the expression of 92 ion channel subunit genes (Table S1). Genes tested included K^+ channels, voltage-dependent Ca^{2+} channels (Cav), epithelial Na^+ channel (ENaC), Cl^- channels, and TRP channels. We detected expression of 60 genes, whose identity and relative abundance are shown in Figure 1. Genes expressed under control conditions included 2 Cl^- channel subunits (CLCN3 and CLCA2); 8 different subunits of inward-rectifier K^+ channels (K_{IR}); 3 two-pore domain K^+ channels (K2P), with highest expression of TREK1 and TWIK1; 7 members of the Ca^{2+} -activated K^+ channels, K(Ca), with larger expression of SK4 and several subunits of the large-conductance Ca^{2+} - and voltage-activated K^+ channel (BK α subunit and accessory subunits $\beta 1$ and $\beta 4$); 7 different voltage-dependent K^+ channel (Kv) β subunits, with prominent expression of KCHIP3, Kv $\beta 1$, and Kv $\beta 2$; 16 different Kv α subunits, with highest expression of Kv7.5, Kv4.1, and Kv4.2; 12 TRP channels; 3 Cav, with high expression of Cav1.2; and 2 ENaC subunits, α and δ .

Changes in uremic serum-treated cells were explored with two methods, hierarchical clustering and gene expression differences. Two genes not initially detected in control cells, Kv1.3 (KCNA3) and the $\beta 2$ subunit of the BK channel (KCNMB2) were detected under uremic conditions. To be able to incorporate these two genes into our analysis we arbitrarily set a Ct value of 40 under control conditions, which will tend to underestimate the differences between conditions. Two-way hierarchical clustering allowed us to group samples following similarities in their expression pattern (Figure 2). We identified two clusters. Cluster A includes genes more robustly expressed in control samples: K(Ca) channels SK2 and SK4; Kv channel subunits Kv $\beta 1$, Kv1.6, and Kv7.5; and TRP channel TRPM7. Cluster B contains genes more abundant in uremic serum-treated samples: chloride channel CLCA2; K_{IR} channel subunits SUR2, Kir2.1, Kir3.1, and Kir6.1; K2P channels TWIK1, TREK1, and TASK1; BK channel α , $\beta 1$, and $\beta 2$ subunits; Kv channel subunits MIRP2, Kv1.3, Kv4.2, and Kv9.1; TRP channels TRPM3, TRPC4, and TRPC6; and the α subunit of ENaC.

To discern whether expression patterns reflect significant associations we studied for each gene the differences in expression between control and uremia. Five days incubation of HASMC with uremic serum-induced statistically significant changes in 17 genes (Figure 3). There was increased expression of the Ca^{2+} -activated Cl^- gene CLCA2, Kir6.1, K2P channels TREK1 and TASK1, BK $\beta 1$, $\beta 2$, and $\beta 4$ (with a particularly large change in $\beta 2$), Kv accessory subunit MIRP2 and α subunits 1.3, 4.2, and 9.1, TRPC4 channel and the ENaC α subunit. Uremic serum reduced expression of K(Ca) channels SK2 and SK4, Kv7.5, and TRPM7 channel (Figure 3).

Kv1.3 Expression Is Altered in the Aorta of a Mouse Model of CKD

Out of the genes modulated by uremic serum, we focused on Kv1.3. Upregulation of Kv1.3 channels has been previously associated with proliferation and phenotypic modulation of VSMC.^{22,27,32} Although our low-density Taqman array suggested a "de novo" expression of Kv1.3 under uremic conditions,²⁵ the expression of this channel has been previously reported in human VSMC cultures.³³ Using a Kv1.3 Taqman probe and conventional qPCR with increased amount of cDNA we were able to detect Kv1.3 expression in control HASMC cultures, which was increased by approximately 10-fold in uremic serum-treated cells (Figure 4A). Association of Kv1.3 with CKD was tested in aorta samples obtained from a mouse model of subtotal (5/6) nephrectomy. Kv1.3 expression in aorta of CKD animals was 10-

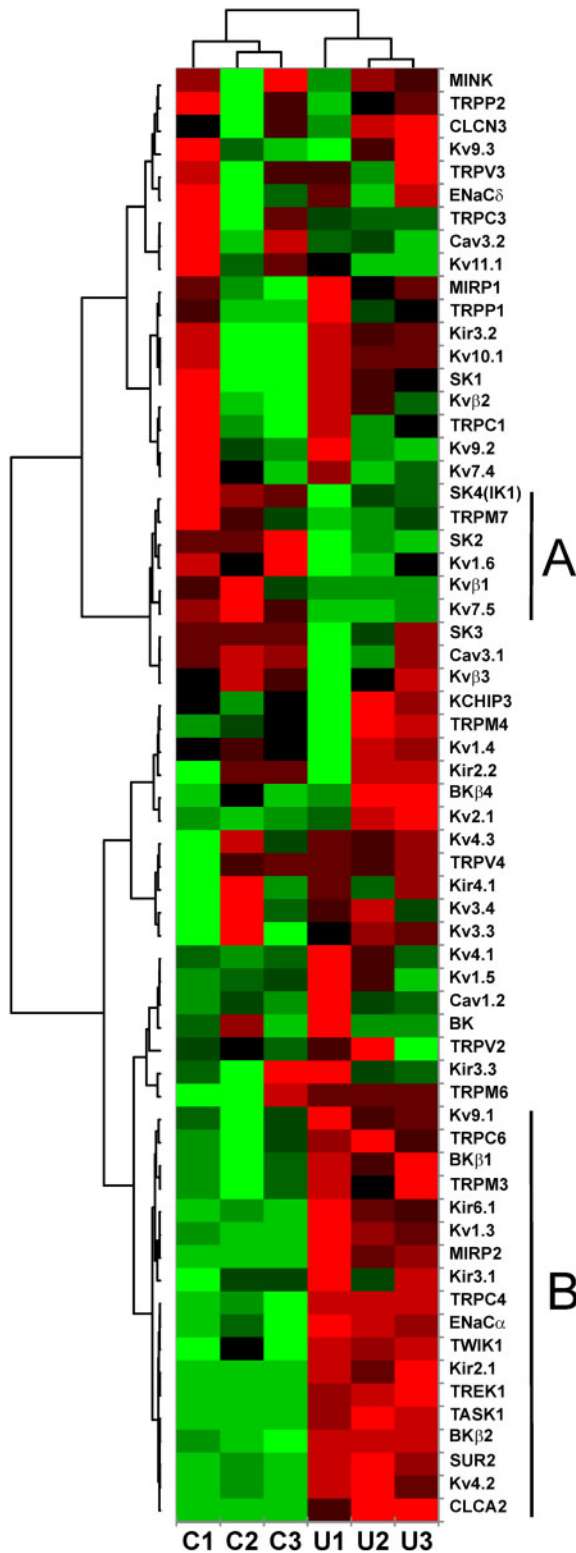


Figure 2. Two-Way Hierarchical Agglomerative Clustering of Ion Channel Subunit Expression in HASMC. The analysis was applied to the 62 genes expressed in HASMC and to three samples treated with control serum (C1 to C3) and three samples treated with uremic serum (U1 to U3). Δ Ct values for each gene and sample were used as input data. A color scale ranging from bright green (lowest) to bright red (highest) represents expression levels for each gene and sample. The length of tree branches is proportional to the correlation of the gene expression pattern. A and B denote the groups of genes most relevant for clustering.

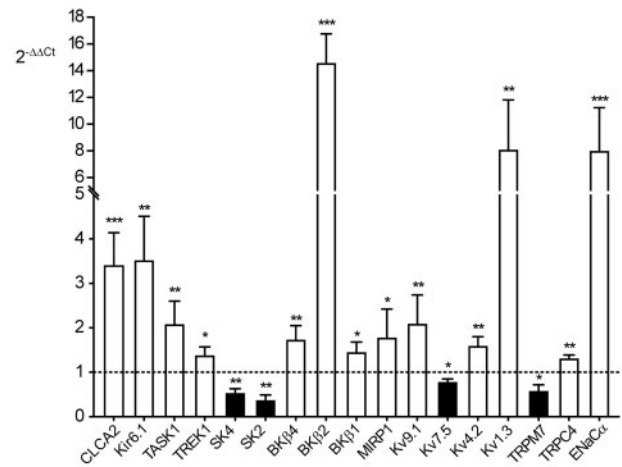


Figure 3. Significantly Altered Ion Channel Subunit Abundance in Cells after Incubation with Uremic Serum. HASMC were cultured in the presence of 20% control or uremic serum for 5 days. Expression changes are expressed as fold-change abundance normalized to GAPDH using the $\Delta\Delta Ct$ method, in HASMC cultured in uremic serum compared to cells cultured in control serum. Open bars represent increased expression in uremic serum; black bars represent decreased expression in uremic serum. Bars are the mean \pm SEM of three independent samples analyzed in duplicate. Student's t-test; * $P < 0.05$; ** $P < 0.01$; *** $P < 0.001$.

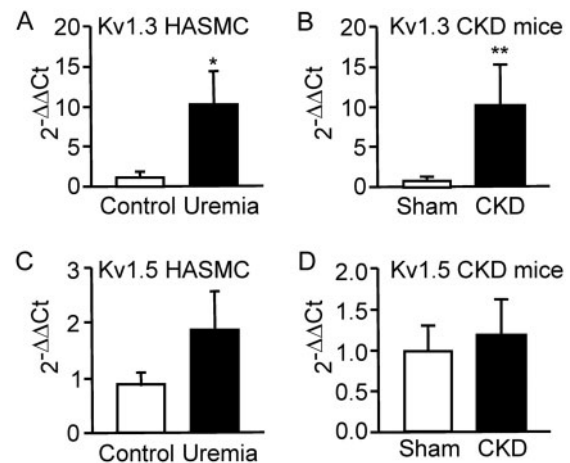


Figure 4. Kv1.3 Channel Abundance Is Upregulated by Uremic Serum in HASMC and in the Aorta of a Mouse Model of CKD. Relative mRNA abundance of Kv1.3 (A and B) and Kv1.5 (C and D) in control or uremic serum-treated HASMC and in aorta from sham-operated and subtotal nephrectomy (5/6 model of CKD) mouse groups. Bars represent mean \pm SEM ($N = 6$). mRNA abundance normalized to GAPDH (HASMC samples) or to HPRT (mouse CKD samples) was calculated as $2^{-\Delta\Delta Ct}$. * $P < 0.05$; ** $P < 0.01$; Student's t-test.

fold higher than in sham-operated controls (Figure 4B). Given that the relative ratio of Kv1.3 and Kv1.5 controls proliferation in glial cells and VSMC,³² we studied Kv1.5 expression both in HASMC and CKD animals. Our results showed that Kv1.5 expression was unaffected by uremic serum (Figure 4C) or in the CKD mice (Figure 4D). Therefore, the ratio of Kv1.3/Kv1.5 is prominently increased by uremia.

Uremic Serum Decreases BK and Total Kv Current Density but Increases the Proportion of Kv1.3-Carried Outward Current

We next explored whether uremia-induced changes in mRNA ion channels expression correlated with changes in the

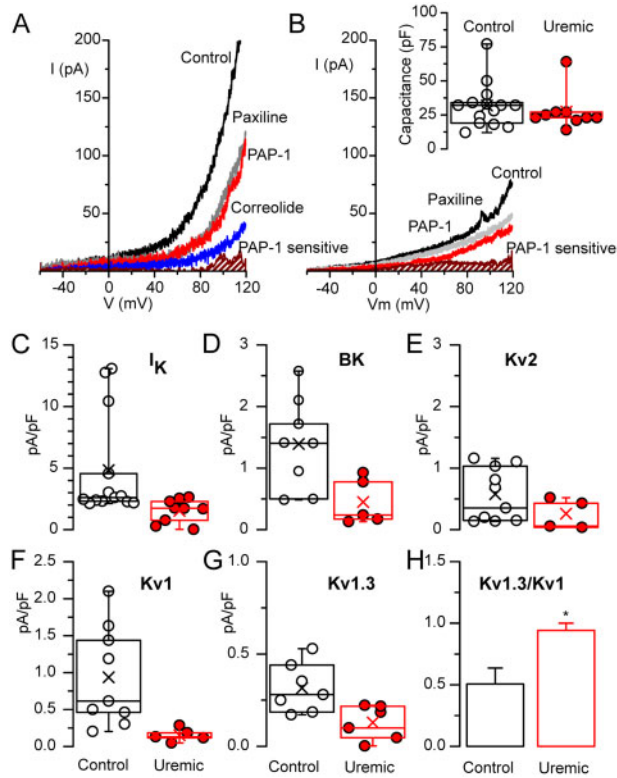


Figure 5. Effects of Uremic Serum on Potassium Current Density. Representative current-voltage (I - V) relationship from patch-clamp recordings obtained in whole-cell configuration under control (A) or uremic serum-treated (B) HASMC before (control traces) and after addition of the indicated inhibitors. Traces were obtained from 2 s depolarizing ramps from -60 to $+120$ mV. In both cases, the PAP-sensitive fraction of the current was obtained by subtracting the current in the presence of PAP-1 from the current in the presence of paxilline. Individual data points and boxplots showing cell capacitances of control and uremic serum-treated cells are shown in the inset. (C) Individual data points and boxplots showing total K^+ current density in HASMC exposed to control or uremic serum. The boxplot range goes from percentile 25 to 75 and whiskers indicate the 5–95 range. Median is represented as a line and media value is shown with an X symbol. $N=9$ –13 individual cells from at least three independent experiments. $^{**}P < 0.01$; MMW test. (D–G) Individual data points and boxplots of the current density carried by BK channels (paxilline-sensitive, D), Kv2 channels (TEA-sensitive, E), Kv1 channels (correlolide-sensitive, F), and Kv1.3 channels (PAP-1-sensitive, G) in HASMC exposed to control (black dots) or uremic serum (red dots). Boxplot representation is as in (C). $N=4$ –10 cells from at least 3 independent experiments. $^{*}P < 0.05$; $^{**}P < 0.01$; MMW test. (H) The bar plots show the fraction of total Kv1 current carried by Kv1.3 channels. Mean \pm SEM ($N=6$ –7). $^{*}P < 0.05$; Student's t -test.

functional expression of the channel proteins. We explored total K^+ , BK, and Kv current densities using whole-cell patch-clamp (Figure 5). Total K^+ current density was significantly decreased by uremic serum (Figure 5C). BK current density (the paxilline-sensitive fraction of outward current³⁴), decreased by 3.2-fold in uremic serum-treated cells (Figure 5D). Both correlolide-sensitive current density (Kv1) and 5-(4-phenoxybutoxy) psoralen (PAP-1)-sensitive current density (Kv1.3) were significantly smaller in HASMC exposed to uremic serum (Figure 5F and G). The contribution of Kv2 and Kv3 channels, identified using 20 mM TEA, also decreased under uremic serum, although the difference was not statistically significant (Figure 5E). However, the fraction of Kv1 currents carried by Kv1.3 increased with uremic serum (Figure 5H), suggesting a larger role for this channel in phenotypically altered HASMC.

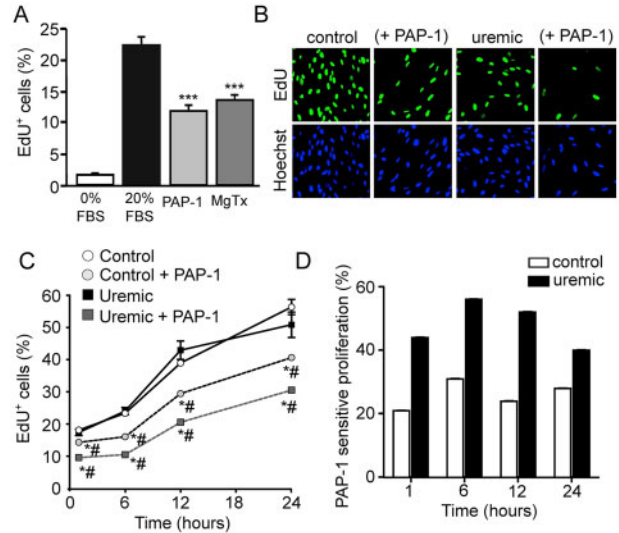


Figure 6. Effects of Kv1.3 Pharmacological Inhibition on HASMC Proliferation. (A) Quantitative analysis of HASMC proliferation. Only 20% FBS-induced proliferation was expressed as the percentage of EdU positive (EdU^+) cells after 6 h incubation. Experimental conditions included the negative control (0% FBS) and the inhibitory effect of PAP-1 (100 nM) and margatoxin (MgTx, 10 nM) on 20% FBS-induced proliferation. Each bar represents mean \pm SEM of 3–4 independent experiments performed in duplicate. Data were analyzed using one-way ANOVA followed by Tukey's test. $^{***}P < 0.001$ vs 20% FBS. (B) Representative micrographs of EdU incorporation in HASMC exposed for 24 h to control or uremic serum in the presence or absence of Kv1.3 inhibitor PAP-1. Nuclei were counterstained with Hoechst 33342 dye. (C) Percentage of EdU^+ cells at the indicated time points after addition of control or uremic serum with or without 100 nM PAP-1. Each data point represents mean \pm SEM (three independent experiments performed in duplicate). Data were analyzed using one-way ANOVA followed by Tukey's test. $^{*}P < 0.05$ vs control; $^{#}P < 0.05$ vs uremic serum. (D) PAP-1-sensitive fraction of EdU incorporation in HASMC treated with control or uremic serum for the indicated period of time.

Kv1.3 Contribution to HASMC Proliferation, Migration, and Calcification under Uremic Conditions

Given the well-established role of Kv1.3 on VSMC proliferation²¹ and the increased contribution of this channel to outward K^+ currents in HASMC after uremic serum treatment (Figure 5), we investigated whether pharmacological inhibition of the channel with PAP-1 alters proliferation under uremic conditions. To ensure the specificity of PAP-1, we compared its effects on HASMC serum-induced proliferation with margatoxin (MgTx), a structurally and mechanically unrelated Kv1.3 inhibitor. Both inhibitors reduced serum-induced HASMC proliferation to the same extent (Figure 6A). When cells were exposed to human control serum, Kv1.3 inhibition significantly decreased proliferation at all time points tested (Figure 6B and C). The effect of PAP-1 was also apparent in HASMC treated with uremic serum (Figure 6B and C). PAP-1 inhibitory effect was significantly larger in HASMC exposed to uremic conditions at all time points explored (Figure 6D). This result indicates that the contribution of Kv1.3 to HASMC proliferation is larger under uremic conditions, consistently with a larger contribution of this channel to Kv1 currents detected in this study.

Our previous characterization of the HASMC model showed that uremic serum potentially decreases cell migration.¹⁰ We used PAP-1 inhibition to test the contribution of Kv1.3 to cell migration and whether this contribution is modified by uremic serum. PAP-1 reduced cell migration up to 50% of the control

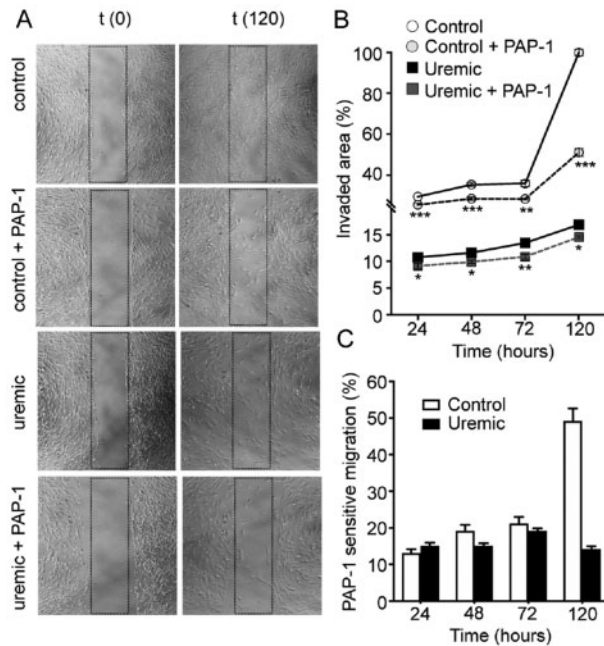


Figure 7. Effects of Kv1.3 Inhibition on HASMC Migration. (A) Representative micrographs of HASMC pretreated for 24 h with control or uremic serum in the presence or absence of 100 nM PAP-1 and placed on serum-free medium to assess cell migration. Pictures were taken at the time of silicon insert removal ($t=0$) or after 120 h. Boxed area indicates the original place of the silicon insert. (B) Graph represents mean (\pm SEM) percentage invaded area at the indicated time points and conditions (three independent experiments performed in triplicate). One-way ANOVA followed by Tukey's test; ** $P < 0.01$; *** $P < 0.001$; **** $P < 0.0001$. (C) PAP-1-sensitive fraction of cell migration in HASMC treated with control or uremic serum for the indicated period of time.

(Figure 7A and B), suggesting a strong dependence of HASMC motility on Kv1.3 function. Cell migration in the presence of uremic serum was drastically reduced, as previously described,¹⁰ with Kv1.3 inhibition further reducing the ability of HASMC to cover the scar by only 15%–20% (Figure 7C).

The possible role of Kv1.3 on uremia-induced calcification was tested by incubating cultured HASMC with control or uremic serum in the presence or absence of PAP-1 for 1 or 5 days. Addition of PAP-1 did not affect basal calcium deposition under control conditions. Treatment of cells with uremic serum induced the expected calcification, which was significantly decreased in cells simultaneously treated with PAP-1 at both time points tested (Figure 8).

Effect of Kv1.3 Blockade or Deletion on Uremia-Induced Calcification on Human and Mouse Vessels in Organ Culture

Finally, we used an ex vivo organ culture model to explore the effect of Kv1.3 on uremia-induced calcification in human and mouse vessels. First, we study the effect of the pharmacological blockade of Kv1.3 with PAP-1 on hMA in organ culture. Vessels were incubated for 10 days with control or uremic serum in the absence or presence of PAP-1. Incubation with 20% FBS medium plus 2.5 mM phosphate (Pi) to induce calcification³⁵ was used as positive control. Alizarin red staining revealed that uremic serum-induced calcification was inhibited by the addition of PAP-1. PAP-1 showed no effect on calcification under control serum conditions (Figure 9A). Then, we study the effect of genetic deletion of Kv1.3 using a Kv1.3 knockout mouse model

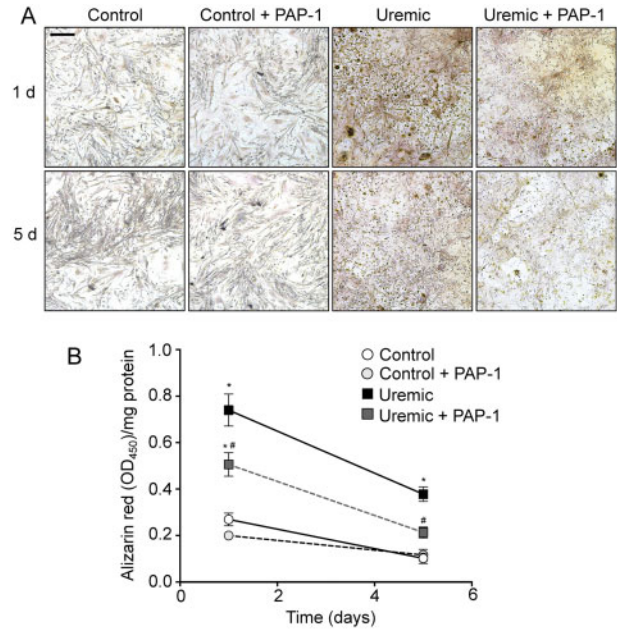


Figure 8. Pharmacological Inhibition of Kv1.3 Channels Reduces Uremia-Induced HASMC Calcification. (A) Representative images of Alizarin Red stained HASMC treated for 24 h or 5 days with control or uremic serum in the presence or absence of 100 nM PAP-1. (B) Quantitation of calcium phosphate deposition by Alizarin Red staining. Each data point represents mean \pm SEM absorbance at 450 nm normalized by the total amount of protein for the indicated day of treatment (three independent experiments, with four replicas per condition in each experiment). Values were compared using Kruskal–Wallis test followed by Dunn's multiple comparisons test. * $P < 0.05$ control vs uremic serum; # $P < 0.05$ vs uremic serum.

(Kv1.3^{-/-}). Aorta arteries from WT and Kv1.3^{-/-} mice were also incubated for 10 days with control and uremic serum. Alizarin staining showed increased calcification in arteries treated with uremic serum from WT mice while arteries from Kv1.3^{-/-} mice were protected from this effect (Figure 9B).

Discussion

Here we studied the effect of serum from uremic patients on the expression of a large panel of ion channel subunits using a previously characterized in vitro human VSMC model.¹⁰ The most dramatic changes were the induction of BK channel $\beta 2$ regulatory subunit and Kv1.3 expression. Kv1.3 channel has been previously characterized as a key player in the phenotypic modulation of VSMC towards a proliferative phenotype.²¹ Following this result, we found that the fraction of Kv1 current carried by Kv1.3 increased in HASMC exposed to uremic serum and that this channel has a larger role in the proliferation of that group compared to control. Most importantly, inhibition of Kv1.3 decreased uremia-induced calcium phosphate deposition both in cultured VSMC and also in a more physiological model, cultured human artery rings. Altogether, these data highlight Kv1.3 channels as a new therapeutic target to prevent uremia-induced calcification associated with CKD. Interestingly, this new target could also improve CKD associated cardiovascular disease, as Kv1.3 blockers are able to prevent intimal hyperplasia in human vessels.²⁵

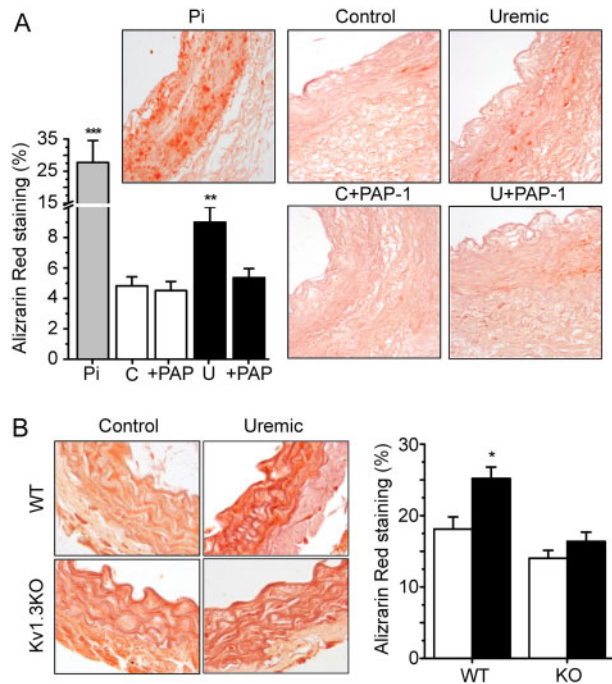


Figure 9. Effects of Pharmacological Inhibition or Genetic Deletion of Kv1.3 on Uremia-Induced Artery Calcification in Organ Culture. (A) Representative images of hMA sections kept in organ culture for 10 days in 20% FBS with 2.5 mM phosphate (Pi, positive control) or in 20% control or uremic serum in the absence or presence of 100 nM PAP-1. Bars show the average percentage of alizarin red-stained area (mean \pm SEM) measured in four different arteries. *** $P < 0.001$ and ** $P < 0.01$ compared with control serum. (B) Representative images of mAs from Kv1.3^{+/+} (WT) and Kv1.3^{-/-} mice kept in organ culture for 10 days in 20% control or uremic serum. Bars show average percentage of stained area (mean \pm SEM) in three arteries. * $P < 0.05$ compare with control serum.

Uremia-Induced Upregulation of Kv1.3 Channels

The Kv expression profile in HASMC is complex, with several subfamilies present at high levels, consistently with previous reports.^{27,33} This profile was relatively unaffected by uremia, with several exceptions, notably the upregulation of Kv1.3. Alteration of Kv1.3 expression during transition from contractile to proliferating phenotype has been previously described.^{21,27,32} Kv1.3 can modulate cell proliferation by several alternative mechanisms, including (1) controlling membrane potential and thus the driving force for Ca^{2+} entry; (2) acting as a voltage sensor that transduces membrane potential into biochemical signals³⁶; (3) altering the channelosome balance relatively to Kv1.5 expression.³² The last two mechanisms have been linked to increased VSMC proliferation after injury. In our in vitro model, uremia-induced expression of Kv1.3 without changes in Kv1.5 mRNA.²⁵ This result was confirmed in the aorta of a mouse model of CKD. Since endothelial cells have low or negligible expression of Kv1, the strongly upregulated Kv1.3 signal detected in our experiment is most likely due to VSMC. In fact, gene expression studies in CKD mouse models demonstrated that uremia directly results in phenotypic modulation of aortic SMCs, leading to a reduction in contractile phenotype markers and vascular contractility.³⁷ Our results showing an increase in the Kv1.3 to Kv1.5 ratio are consistent with uremia-induced phenotypic modulation.^{25,30} This suggests that modified Kv1.3 expression could be an early alteration during the evolution of CKD. In addition, the proportion of total Kv1 current carried by Kv1.3 in HASMC increased, strongly suggesting that the aforementioned

mechanisms could play a role during uremia. Consistently, our data show that Kv1.3 blockade inhibits HASMC proliferation both under control and uremic-serum treatment. Remarkably, although uremia does not have significant effects on cell proliferation, the contribution of the Kv1.3 channels is larger when the uremic serum is used as stimulus (Figure 6).

The VSMC phenotypic switch is also characterized by Kv1.3-regulated increase in cell migration.^{25,27} In our model, uremic serum strongly reduces cell migration and the relative contribution of Kv1.3 under these conditions is time dependent (Figure 7). Control cells migrate enough after 120 h to completely fill up the wounded area in the scratch assay, and this response is heavily dependent on Kv1.3 activity (~50%). On the contrary, uremic serum-treated cells barely recover ~15% of the wounded area, and such effect is almost Kv1.3 insensitive in spite of having higher levels of Kv1.3 expression. It is interesting to point out that uremic serum has an almost opposite effect on the role of Kv1.3 channels in proliferation and migration, indicating the presence in the uremic serum of some yet unidentified factors that counteract Kv1.3 effects on migration.

Additionally, our data showed that Kv1.3 inhibition partially reverts uremia-induced calcification in HASMC and more remarkably, in cultured hMA rings. The role of Kv1.3 in this process is endorsed when uremia-induced calcification is studied in a Kv1.3^{-/-} mouse. Uremic serum induces calcification in cultured WT aorta rings, but this effect is absent in aorta rings from Kv1.3^{-/-}. These results validate Kv1.3 as potential therapeutic target against calcification, and consolidate the general notion that targeting Kv1.3 can be used in a number of different human pathologies.³⁸⁻⁴⁰

Mechanisms of Kv1.3 Channel Effects in Uremia

Calcification is a highly complex and regulated process that implicates both apoptosis/necrosis of VSMC⁷⁻⁹ and the switch to an osteochondrogenic phenotype.^{4,10-12} We previously detected a moderate increase in necrosis and apoptosis when HASMC was treated with uremic serum.¹⁰ In addition, uremia induced a clear upregulation of molecular markers of osteochondrogenic differentiation,¹⁰ suggesting that both mechanisms play a role in calcification. Inhibition of mitochondria-associated Kv1.3 has been shown to induce apoptosis in glioblastoma cells,⁴¹ although it is unclear whether this phenomenon also applies to VSMC. A different type of Kv, Kv7.3, has been recently implicated in osteoblast differentiation and mineralization.⁴² However, expression of Kv1.3 has not been reported in osteoblasts or chondrocytes, nor any contribution to phosphate transport or mineralization, although this does not rule out the possibility that the channel may contribute to the transdifferentiation process.

Phenotypic modulation of VSMC seems to be a prerequisite for uremic calcification. Among the signaling pathways which contribute to the proliferative, migratory, and secretory phenotype of VSMC, PI3K/Akt, and MEK/ERK pathways have been reported to be involved in multiple VSMC preparations, both in vivo and in vitro. We have previously described that MEK/ERK signaling pathway is involved in Kv1.3 induced VSMC proliferation, as Kv1.3 effect on proliferation can be inhibited by Kv1.3 blockers and MEK blockers, being these effects non-additive.³⁰ There are evidences supporting a critical role of MEK/ERK activation in vascular calcification in CKD,⁴³ so that the effects of Kv1.3 on uremic calcification could be mediated by Kv1.3-induced pERK activation.

In any case, there is a big number of putative toxins in the uremic serum⁴⁴ that could be responsible for Kv1.3 upregulation and that could differentially modulate the signaling pathways in which channels are involved (proliferation, migration, calcification). Dissecting the candidates would be relevant, not only from a translational perspective, but also as a way of defining more precisely the molecular mechanisms involved in Kv1.3 function in the vascular wall.

Uremia-Induced Changes in Other Ion Channels Expression

BK channels couple cytosolic Ca²⁺ signaling with the control of membrane potential, constituting a key regulatory mechanism in smooth muscle contraction.⁴⁵ Our transcriptional profiling detected uremia-induced increased abundance of the BK regulatory β subunits, particularly a 15-fold increase in β 2, without changes in the pore-forming α subunit. β 2 induces inactivation of BK channels,^{46,47} which is consistent with the detected decreased in paxilline-sensitive current density. Moreover, as BK channels do not contribute to human VSMC proliferation,³⁰ we did not explore the role of this channel any further. Transcriptional profiling also revealed decreased abundance of K(Ca) channel subunits SK2 and SK4. While they are abundant and highly relevant in endothelial cells, the expression and functional relevance of SK1-3 channels in VSMC are unclear.⁴⁸ In contrast, SK4 upregulation has been previously implicated in the control of VSMC proliferation both in vivo and in vitro.^{22,27,49} Downregulation of SK4 expression in cells treated with uremic serum could fit our previous report showing that uremic serum induces severe changes in cytosolic Ca²⁺ handling, with loss of receptor-operated responses and depletion of intracellular stores.¹⁰ Blockade of SK4 leads to decreased VSMC proliferation and migration.^{49,50} However, inhibition of VSMC proliferation by SK4 blockers in human VSMCs does not potentiate the effect of Kv1.3 channel blockers, suggesting the contribution through some common effectors to ensure proliferation upon phenotypic modulation.³⁰ Consistently with those previous observations, here we found that uremic serum (which simultaneously upregulates Kv1.3 and downregulates SK4) does not affect the overall proliferation rate of HASMC but increases the Kv1.3-dependent fraction.

Regarding Cav channels, injury to the vascular wall typically induces a phenotypic modulation from contractile to a proliferative state accompanied by loss of L-type channels and increased expression of T-type channels,⁵¹ although this is not detected in all preparations.²⁷ In HASMC, uremia did not alter expression or induced other types of Cav, suggesting that this treatment does not bring a classic proliferative state. This idea is further supported by the lack of clearly enhanced expression of the TRPC family of ion channels or upregulation of SK4 in uremic serum-treated HASMC, opposite to what has been described in the classical switch between contractile and proliferative phenotypes.⁵¹

Concluding Remarks

The uremic serum from patients with reduced kidney function modulates the phenotype of VSMCs and promotes vascular calcification a condition strongly associated with cardiovascular risk. Several molecules of uremic serum have already been linked to vascular calcification but the complexity of this milieu suggests that there is not a single molecule implicated in this complex process.⁴⁴ Deciphering the mechanisms and key

elements involved in this phenomenon will provide valuable information to reduce the cardiovascular risk linked to CDK.

Our results showed that uremic serum-induced ion channel expression remodeling in HASMC is distinct from the remodeling accompanying the phenotypic modulation from contractile to proliferative phenotypes. Some of these changes, together with the previously described loss of receptor-operated cytosolic Ca²⁺ signaling,¹⁰ are consistent with a loss of excitability. Most importantly, enhanced expression of Kv1.3 mRNA led to increased function of this channel, which, in addition to its role in cell proliferation and migration, also appears to be implicated in uremia-induced calcification. Additional studies are needed to understand the mechanisms linking Kv1.3 to cell calcification and whether this process is relevant in vivo.

Acknowledgments

We would like to thank Esperanza Alonso for excellent technical assistance, Natalia Serrano-Morillas for performing qPCR experiments on HASMC, and Sara Moreno-Estar and Marycarmen Arévalo for help with vessel calcification studies. We acknowledge cofunding by Fondo Europeo de Desarrollo Regional (FEDER). J.F.N.-G. is member of the ISCIII-RETIC-REDINREN (RD16/0009/0022).

Supplementary Material

Supplementary material is available at the APS Function online.

Funding

This work was funded by grants BFU2016-78374-R (to D.A.d.l.R.) and BFU2016-75360-R (to J.R.L.-L. and M.T.P.-G.) from the Ministerio de Economía y Competitividad (MINECO, Spain), grant PI13/01726 (to J.F.N.-G.) from the Instituto de Salud Carlos III (ISCIII, MINECO), European Research Council, under Horizon 2020 Research and Innovation Programme Grant (ERC-CoG-2014 648936) to T.G., grant RTI2018-098768-B-I00 from Spanish Ministerio de Ciencia, Innovación y Universidades to T.G., and grant VA114P17 (Junta de Castilla y León) to M.T.P.-G. T.G. was supported by Programa Ramon y Cajal (RYC-2012-11349, MINECO).

Conflict of Interest Statement

The authors declare that they do not have competing interests.

Authors' Contributions

V.C.-P. performed experiments, analyzed data, interpreted results, prepared figures, and participated in drafting the manuscript. P.C. performed experiments, analyzed data, and interpreted results. J.F.N.-G. selected the patients and participated in the study design. J.R.-M. performed experiments and analyzed data. F.J. performed experiments, analyzed data, and interpreted results. J.R.L.-L. analyzed data and interpreted results of experiments. D.A.d.l.R. participated in the study design, analyzed data, interpreted results, and participated in drafting the manuscript. M.T.P.-G.

performed experiments, analyzed data, interpreted results participated in drafting the manuscript. T.G. participated in the study design, analyzed data, interpreted results, and drafted the manuscript. All authors revised the manuscript and approved its final version.

References

1. Tonelli M, Pfeffer MA. Kidney disease and cardiovascular risk. *Annu Rev Med* 2007;58:123–39.
2. Provenzano M, Coppolino G, De Nicola L, et al. Unraveling cardiovascular risk in renal patients: a new take on old tale. *Front Cell Dev Biol* 2019;7:314.
3. Benz K, Varga I, Neureiter D, et al. Vascular inflammation and media calcification are already present in early stages of chronic kidney disease. *Cardiovasc Pathol* 2017;27:57–67.
4. Moe SM, Chen NX. Pathophysiology of vascular calcification in chronic kidney disease. *Circ Res* 2004;95(6):560–7.
5. Chen NX, Duan D, O'Neill KD, et al. The mechanisms of uremic serum-induced expression of bone matrix proteins in bovine vascular smooth muscle cells. *Kidney Int* 2006;70(6):1046–53.
6. Viegas CSB, Santos L, Macedo AL, et al. Chronic kidney disease circulating calciprotein particles and extracellular vesicles promote vascular calcification: a role for GRP (Glrich protein). *Arterioscler Thromb Vasc Biol* 2018;38(3):575–87.
7. Proudfoot D, Skepper JN, Hegyi L, Bennett MR, Shanahan CM, Weissberg PL. Apoptosis regulates human vascular calcification in vitro: evidence for initiation of vascular calcification by apoptotic bodies. *Circ Res* 2000;87(11):1055–62.
8. Shroff RC, McNair R, Figg N, et al. Dialysis accelerates medial vascular calcification in part by triggering smooth muscle cell apoptosis. *Circulation* 2008;118(17):1748–57.
9. Clarke MC, Littlewood TD, Figg N, et al. Chronic apoptosis of vascular smooth muscle cells accelerates atherosclerosis and promotes calcification and medial degeneration. *Circ Res* 2008;102(12):1529–38.
10. Cazaña-Perez V, Cidad P, Donate-Correa J, et al. Phenotypic modulation of cultured primary human aortic vascular smooth muscle cells by uremic serum. *Front Physiol* 2018;9:89.
11. Chen NX, Duan D, O'Neill KD, Moe SM. High glucose increases the expression of Cbfa1 and BMP-2 and enhances the calcification of vascular smooth muscle cells. *Nephrol Dial Transplant* 2006;21(12):3435–42.
12. Chang JF, Liu SH, Lu KC, et al. Uremic vascular calcification is correlated with oxidative elastic lamina injury, contractile smooth muscle cell loss, osteogenesis, and apoptosis: the human pathobiological evidence. *Front Med (Lausanne)* 2020;7:78.
13. Bostrom K, Watson KE, Horn S, Wortham C, Herman IM, Demer LL. Bone morphogenetic protein expression in human atherosclerotic lesions. *J Clin Invest* 1993;91(4):1800–9.
14. Demer LL. Vascular calcification and osteoporosis: inflammatory responses to oxidized lipids. *Int J Epidemiol* 2002;31(4):737–41.
15. Rogers M, Goettsch C, Aikawa E. Medial and intimal calcification in chronic kidney disease: stressing the contributions. *J Am Heart Assoc* 2013;2(5):e000481.
16. Schwarz U, Buzello M, Ritz E, et al. Morphology of coronary atherosclerotic lesions in patients with end-stage renal failure. *Nephrol Dial Transplant* 2000;15(2):218–23.
17. Smith ER. Vascular calcification in uremia: new-age concepts about an old-age problem. *Methods Mol Biol* 2016;1397:175–208.
18. Durham AL, Speer MY, Scatena M, Giachelli CM, Shanahan CM. Role of smooth muscle cells in vascular calcification: implications in atherosclerosis and arterial stiffness. *Cardiovasc Res* 2018;114(4):590–600.
19. Kaplan-Albuquerque N, Bogaert YE, Van Putten V, Weiser-Evans MC, Nemenoff RA. Patterns of gene expression differentially regulated by platelet-derived growth factor and hypertrophic stimuli in vascular smooth muscle cells: markers for phenotypic modulation and response to injury. *J Biol Chem* 2005;280(20):19966–76.
20. Jackson WF. Potassium channels in regulation of vascular smooth muscle contraction and growth. *Adv Pharmacol* 2017;78:89–144.
21. Lopez-Lopez JR, Cidad P, Perez-Garcia MT. Kv channels and vascular smooth muscle cell proliferation. *Microcirculation* 2018;25(1). doi: 10.1111/micc.12427.
22. Cidad P, Novensa L, Garabito M, et al. K⁺ channels expression in hypertension after arterial injury, and effect of selective Kv1.3 blockade with PAP-1 on intimal hyperplasia formation. *Cardiovasc Drugs Ther* 2014;28(6):501–11.
23. Schmitz A, Sankaranarayanan A, Azam P, et al. Design of PAP-1, a selective small molecule Kv1.3 blocker, for the suppression of effector memory T cells in autoimmune diseases. *Mol Pharmacol* 2005;68(5):1254–70.
24. Cidad P, Jimenez-Perez L, Garcia-Arribas D, et al. Kv1.3 channels can modulate cell proliferation during phenotypic switch by an ion-flux independent mechanism. *Arterioscler Thromb Vasc Biol* 2012;32(5):1299–307.
25. Arevalo-Martinez M, Cidad P, Garcia-Mateo N, et al. Myocardin-dependent Kv1.5 channel expression prevents phenotypic modulation of human vessels in organ culture. *Arterioscler Thromb Vasc Biol* 2019;39(12):e273–86.
26. Yang HC, Zuo Y, Fogo AB. Models of chronic kidney disease. *Drug Discov Today Dis Models* 2010;7(1–2):13–19.
27. Cidad P, Moreno-Dominguez A, Novensa L, et al. Characterization of ion channels involved in the proliferative response of femoral artery smooth muscle cells. *Arterioscler Thromb Vasc Biol* 2010;30(6):1203–11.
28. Moreno-Dominguez A, Cidad P, Miguel-Velado E, Lopez-Lopez JR, Perez-Garcia MT. De novo expression of Kv6.3 contributes to changes in vascular smooth muscle cell excitability in a hypertensive mice strain. *J Physiol* 2009;587(3):625–40.
29. Schmittgen TD, Livak KJ. Analyzing real-time PCR data by the comparative C(T) method. *Nat Protoc* 2008;3(6):1101–8.
30. Cidad P, Miguel-Velado E, Ruiz-McDavitt C, et al. Kv1.3 channels modulate human vascular smooth muscle cells proliferation independently of mTOR signaling pathway. *Pflugers Arch* 2015;467(8):1711–22.
31. Schneider CA, Rasband WS, Eliceiri KW. NIH Image to ImageJ: 25 years of image analysis. *Nat Methods* 2012;9(7):671–5.
32. Perez-Garcia MT, Cidad P, Lopez-Lopez JR. The secret life of ion channels: Kv1.3 potassium channels and proliferation. *Am J Physiol Cell Physiol* 2018;314(1):C27–42.
33. Miguel-Velado E, Moreno-Dominguez A, Colinas O, et al. Contribution of Kv channels to phenotypic remodeling of human uterine artery smooth muscle cells. *Circ Res* 2005;97(12):1280–7.
34. Li G, Cheung DW. Effects of paxilline on K⁺ channels in rat mesenteric arterial cells. *Eur J Pharmacol* 1999;372(1):103–7.
35. Akiyoshi T, Ota H, Iijima K, et al. A novel organ culture model of aorta for vascular calcification. *Atherosclerosis* 2016;244:51–58.
36. Cidad P, Alonso E, Arevalo-Martinez M, et al. Voltage-dependent conformational changes of Kv1.3 channels activate cell proliferation. *J Cell Physiol* 2020. doi: 10.1002/jcp.30170.

37. Madsen M, Aarup A, Albinsson S, et al. Uremia modulates the phenotype of aortic smooth muscle cells. *Atherosclerosis* 2017; 257:64–70.
38. Perez-Verdaguer M, Capera J, Serrano-Novillo C, Estadella I, Sastre D, Felipe A. The voltage-gated potassium channel Kv1.3 is a promising multitherapeutic target against human pathologies. *Expert Opin Ther Targets* 2016;20(5):577–91.
39. Kazama I, Tamada T. Lymphocyte Kv1.3-channels in the pathogenesis of chronic obstructive pulmonary disease: novel therapeutic implications of targeting the channels by commonly used drugs. *Allergy Asthma Clin Immunol* 2016;12:60.
40. Kazama I. Physiological significance of delayed rectifier K(+) channels (Kv1.3) expressed in T lymphocytes and their pathological significance in chronic kidney disease. *J Physiol Sci* 2015;65(1):25–35.
41. Leanza L, Romio M, Becker KA, et al. Direct pharmacological targeting of a mitochondrial ion channel selectively kills tumor cells in vivo. *Cancer Cell* 2017;31(4):516–31.e510.
42. Yang JE, Song MS, Shen Y, Ryu PD, Lee SY. The role of KV7.3 in regulating osteoblast maturation and mineralization. *Int J Mol Sci* 2016;17(3):407.
43. Huang M, Zheng L, Xu H, et al. Oxidative stress contributes to vascular calcification in patients with chronic kidney disease. *J Mol Cell Cardiol* 2020;138:256–68.
44. Rapp N, Evenepoel P, Stenvinkel P, Schurgers L. Uremic toxins and vascular calcification-missing the forest for all the trees. *Toxins (Basel)* 2020;12(10). doi: 10.3390/toxins12100624.
45. Nelson MT, Cheng H, Rubart M, et al. Relaxation of arterial smooth muscle by calcium sparks. *Science* 1995;270(5236): 633–7.
46. Wallner M, Meera P, Toro L. Molecular basis of fast inactivation in voltage and Ca²⁺-activated K⁺ channels: a transmembrane beta-subunit homolog. *Proc Natl Acad Sci USA* 1999;96(7):4137–42.
47. Xia XM, Ding JP, Lingle CJ. Molecular basis for the inactivation of Ca²⁺- and voltage-dependent BK channels in adrenal chromaffin cells and rat insulinoma tumor cells. *J Neurosci* 1999;19(13):5255–64.
48. Marchenko SM, Sage SO. Calcium-activated potassium channels in the endothelium of intact rat aorta. *J Physiol* 1996; 492(Pt 1):53–60.
49. Kohler R, Wulff H, Eichler I, et al. Blockade of the intermediate-conductance calcium-activated potassium channel as a new therapeutic strategy for restenosis. *Circulation* 2003;108(9):1119–25.
50. Tharp DL, Wamhoff BR, Wulff H, Raman G, Cheong A, Bowles DK. Local delivery of the KCa3.1 blocker, TRAM-34, prevents acute angioplasty-induced coronary smooth muscle phenotypic modulation and limits stenosis. *Arterioscler Thromb Vasc Biol* 2008;28(6):1084–9.
51. House SJ, Potier M, Bisailon J, Singer HA, Trebak M. The non-excitable smooth muscle: calcium signaling and phenotypic switching during vascular disease. *Pflugers Arch* 2008;456(5): 769–85.